JAAS

Accepted Manuscript

This is an *Accepted Manuscript*, which has been through the Royal Society of Chemistry peer review process and has been accepted for publication.

Accepted Manuscripts are published online shortly after acceptance, before technical editing, formatting and proof reading. Using this free service, authors can make their results available to the community, in citable form, before we publish the edited article. We will replace this *Accepted Manuscript* with the edited and formatted *Advance Article* as soon as it is available.

You can find more information about *Accepted Manuscripts* in the Information for Authors.

Please note that technical editing may introduce minor changes to the text and/or graphics, which may alter content. The journal's standard Terms & Conditions and the Ethical guidelines still apply. In no event shall the Royal Society of Chemistry be held responsible for any errors or omissions in this *Accepted Manuscript* or any consequences arising from the use of any information it contains.

ROYAL SOCIETY OF CHEMISTRY

www.rsc.org/jaas

Handheld energy-dispersive X-ray fluorescence spectrometry on carbonate: opportunities and challenges

Jennifer Quye-Sawyer, Veerle Vandeginste*, Kimberley Johnston†

Department of Earth Science and Engineering, Imperial College London, London SW7 2BP, UK

*Corresponding author: v.vandeginste@imperial.ac.uk

†Deceased 27 February 2015

Abstract

Technology development over the last years has led to significant improvements in the quality and flexibility of portable instruments. Notably, handheld energy-dispersive X-ray fluorescence (ED-XRF) spectrometry has seen a bloom both in terms of technical development and applications, ranging from the field of mineral exploration to archaeology, environmental science, paleoclimatology and forensic science. However, the field of carbonate geoscience has not yet taken the capability and flexibility of this tool to its advantage. This study developed a methodology for the application of handheld XRF on carbonate. An assessment was made in terms of measurement time, sample preparation and weathering of outcrops. Correction equations are presented for elemental concentrations of Ca, Ti, Fe, Mn, Zn, Al, K, Mg, Ba, Sr, Rb and Si that were derived from calibration based on a series of carbonate lab standards. Weathering can pose a significant issue for in situ measurements on field carbonate outcrops, since weathering impacts on the concentrations of Ca, Mg, Ti and Al in the carbonate rocks. Therefore, we advise that XRF is used on fresh rock chips that are hammered from the carbonate outcrop to take advantage of making measurements in situ and at the same hand ensuring reliable quantitative results. This method allows a rapid and inexpensive geochemical characterization of carbonate, which opens opportunities for stratigraphic, sedimentological, paleoenvironmental and diagenetic studies in extensive study areas.

Keywords

limestone, dolomite, geochemistry, handheld XRF, major elements, trace elements.

Introduction

X-ray fluorescence is a well-established analytical technique, which allows the measurement of the composition of a sample using emission spectra (after excitation of electrons by incident X-radiation) which are characteristic for atoms of specific elements [1]. In recent years portable XRF has become a widespread method for quick and non-destructive analysis of geological materials. Modern handheld instruments are reported to achieve very similar accuracy and precision to larger XRF instruments [2], which means that samples which do not need lab sample preparation no longer need to be taken to the lab for analysis. Recent applications of portable XRF include mineral exploration [3, 4], meteorite research [5, 6], detection of metallic contaminants in water and soil [7-11], archaeological identification of obsidian [2, 12-16] and glass [17-20], gemstone provenance [21], compositional analysis of bronze artefacts (Vittiglio et al, 1999), paleoclimate studies on mudrocks [22, 23], bill characterization in forensic science [20] and other applications such as heavy metals in automative brake linings [24].

The use of field-portable XRF on carbonates, however, is not yet fully exploited. Apart from a publication from 1999, with XRF equipment which is in the meantime outdated [25], no research has been published in peer-reviewed international journals on handheld or portable X-ray fluorescence spectrometry on carbonate, as far as the authors are aware of. The truly portable nature of handheld XRF instruments creates carbonate research opportunities not only in the field of earth sciences but also in the growing field of conservation of limestone buildings [26-28], where destructive testing is undesirable. It is known that XRF values strongly depend on the matrix [29], but also on the surface morphology [30, 31], as well as the sensitivity of the instrument [1] and several XRF manufacturer provide calibrations specific to certain types of material. However, these calibrations need to be tested and adapted for the use of new materials, and, hence, a calibration or correction needs to be developed for the use of XRF on carbonate. In this study, we develop a correction for elements that have significant concentrations above the XRF detection limit that is applied on top of the mudrock calibration

provided by the manufacturer. An additional goal of this study is to test the impact of several parameters of sample type and preparation on the XRF values and the impact of weathering and practicality of using the XRF in situ on carbonate outcrops.

Material and Methodology

The instrumentation used was a handheld Bruker Tracer IV-SD (ED-XRF) and a Bruker 3V Vacuum Pump. The handheld XRF uses a rhodium target and is equipped with a Silicon Drift Detector to aid detection of the lighter elements. All the carbonate samples were analysed using both the Trace Mud Rock (TMR) and Major Mud Rock (MMR) modes, which operate at 40kV and 15kV respectively. Theoretically, TMR can determine 50 elements (Mg, Al, Si, P, S, Cl, K, Ca, Sc, Ti, V, Cr, Mn, Fe, Co, Ni, Cu, Zn, As, Se, Br, Rb, Sr, Y, Zr, Nb, Mo, Ru, Rh, Pd, Ag, Cd, In, Sn, Sb, Te, I, Ba, Hf, Ta, W, Re, Os, Ir, Pt, Au, Pb, Bi, Th and U). MMR also determines 50 elements (as for TMR but including Na and excluding Th). A vacuum pump was used for the analyses. Vacuum conditions help preventing the absorption of low energy radiation by air within the tube, which would hinder the detection of light elements [32].

Cross-validation presented in this paper compares mass spectrometry (MS) concentrations with values obtained by XRF using MMR and TMR settings, which are calibrations of raw XRF spectra for mudrock using influence coefficient algorithms [23]. Subsequently, linear or quadratic regression lines are presented for specific elements to calibrate the TMR or MMR reported XRF values for their true value in carbonates. Thirty-eight reference standards were used for this calibration (Table 1). These include two international reference standards, GBW-07114 and BCS CRM No. 393, whereas the other, in-house reference standards are mainly carbonate samples (limestone, dolomite, partially dolomitized limestone, diagenetic calcite and also a barite sample and a dolomite sample containing gypsum) collected over the years from a wide range of geographical locations, geological age and from both outcrop and drill cores. The samples were powdered by hand using an agate or porcelain mortar and pestle. Accurate values of the major and trace element composition in these standards were obtained using ICP-MS and ICP-AES by SGS Mineral Services (Canada) using the sodium

peroxide fusion technique (SGS method ICM90A). Values obtained by the latter method are referred to as "MS data" in the text below. Measurements for cross-validation using the XRF on these standards were carried out on powders (of about 3g) within plastic sample cups coated with 4µm thick Prolene film. A measurement time of 120 seconds was used for both MMR and TMR settings. XRF values used for the cross-validation are the average values of triplicate measurements on all standards. Between each replicate the sample cup was shaken to redistribute the powder and assess homogeneity and reproducibility.

As reported in the results, the impact of measurement time, thin film and sample preparation on the XRF values was evaluated on several standards. To determine the potential impact on XRF readings caused by sample preparation differences, the following preparation methods were employed: polished rock surfaces using silicon carbide compound at 220 and 600 grit sizes, sieved powder sizes, rough hammered fresh rock surfaces and weathered rock surfaces.

Results

XRF measurement time

A certified dolomite reference standard JDo-1 was used to evaluate the impact of measurement time, tested for 30, 60, 120 and 180 seconds. Measurements were performed on the fine powder in a sample cup covered by 4µm thin Prolene film. The measurement standard error decreases with increasing measurement time for each element (Fig. 1A). Reproducibility of the measurements is evaluated by the relative standard deviation of triplicate measurements of the reference standard for different measurement times. For most elements, the relative standard deviation decreases significantly from 30 to 60 seconds measurements time and still decreases significantly for Si from 60 to 120 seconds measurement (Fig. 1B). There is significant variation in the ratio for the element Mg for different measurement times and a lack of decrease in the relative standard deviation with longer measurement time for Fe and Mn (Fig. 1B). Also other elements detected by XRF did not show significant improvement in relative standard deviation with longer measurement time.

Sample Preparation

Thin film

Powder samples are placed in a sample cup and covered with thin film. Two types of film were compared, Chemplex SpectroCertified Prolene 4µm thin film and Mylar X-ray 1.5µm thin film. The impact on the type of thin film used was assessed by XRF measurements on the films as blanks, both as single thin film on empty sample cup and as thick package of thin film on a thin film roll. Significant differences between the concentration of elements measured in MMR and TMR mode are recorded for Si and S, which have higher values in the Mylar thin film than the Prolene film, and for V, which has higher concentrations in the Prolene film than the Mylar film. These differences are higher than the internal error for the measurement and higher than the standard deviation for the triplicates of measurements on the thin films, and thus considered as significant. Concentrations for all three elements are based on the MMR setting and presented in %; the concentrations are 0.967 ± 0.016 and 0.841 ± 0.013 for Si, 0.127 ± 0.005 and 0.102 ± 0.005 for S and 0.0010 ± 0.0003 and 0.0019 ± 0.0003 for V, for Mylar single thin film and Prolene single thin film respectively. All other elements are either below the detection limit or do not show a significant difference between the Mylar and Prolene films.

Grain size of powdered rock

A calcite crystal, and also a barite crystal (barium sulphate) for comparison, was first grinded and subsequently sieved to separate the 63 to 125µm and the 125 to 250µm grain size fractions. XRF measurements are very similar for the two size fractions on calcite and barite. Generally, the measured elemental concentrations fall within 3ppm of each other or below 1% of the average value. Larger differences (relative standard deviation) have been observed for Ba (88%), Fe (6%), K (9%), Sr (12%) and Ti (17%) in calcite and for Al (3%), Ca (18%), Cr (9%), Sr (2%) and P (3%) in barite. The only two elements that show a consistent change between measurements on different grain size fractions for calcite and barite are Ba and Sr. In both cases, the elemental concentration is lower for the coarser size fraction. The difference for these elements falls within 2% in barite, but is significantly higher in calcite, as reported above.

Polished, rough fresh and weathered rock samples

The impact of the roughness and weathering state of the sample was evaluated by comparison with powder of the same sample. Therefore, several samples were prepared in different ways, i.e. polished with silicon carbide grit 600 (fine polish), grit 220 (coarser polish), rough fresh surface by breakage due to hammering and unprepared surface that had been exposed to some degree of weathering. Results show that the Ca concentration of weathered rock surfaces is significantly lower than that measured on polished or fresh rock surfaces and in powder; this results in a offset of about 10% Ca (Fig. 2). The Mg concentration shows an increased value on polished rock surfaces (about double) compared to the readings on powder, whereas fresh rough and especially weathered rock surfaces display depleted values compared to the signature in the powder (Fig. 2). Al and Ti both show higher values for weathered rock surfaces than in powder samples. Also Fe and Mn show enriched values in weathered and fresh rough rock surfaces than in powder, especially for samples with concentrations of more than a few % Fe and more than 0.5% Mn (Fig. 2). Enrichments are in the order of 2 to 4% for Fe and 0.3% for Mn. The Sr concentration is quite similar between different sample preparation types, except for two outliers for polished grit 600 samples (Fig. 2). Other elements do not show significant differences between different preparation types or were not considered due to lack of cross-validation (see next section).

Cross-validation procedure

MS data quality

Two certified reference standards (in powder form and measured in sample cup covered by 4µm Prolene thin film), one limestone CRM No. 393 and one dolomite GBW 07114, were used within the selection of samples used for calibration of the XRF data versus MS data. These reference standards thus allow assessment on the quality of the MS data. The limestone standard is only certified for the major elements, whereas the dolomite standard is also characterized for minor and trace elements. It is clear that MS data show a much closer fit to the certified concentrations than the XRF data (Fig. 3). The largest offset is observed for K, which is significantly overestimated by MS (0.1% for both)

compared to the certified value of 0.008% for limestone and 0.016% for dolomite. Also the Al concentration is overestimated by MS data (0.06% for both) compared to the certified value of 0.032% for limestone and 0.026% for dolomite. The fact that the linear trend curve suggests an underestimate of the MS values compared to the certified values for the limestone standard (slope of 0.95; Fig. 3) relates to an underestimated value for Ca, i.e. 37.5% versus the certified value of 39.6%

XRF MMR versus TMR data compared with MS data

Several elements are detected by XRF both in the MMR and TMR settings. However, correlation between those data and the MS data can be significantly different between MMR and TMR data (Fig. 4). Also significant differences in the absolute data are observed. For the total set of samples measured in this study, the MMR setting results in more accurate and precise data for Ca and Ti, whereas the TMR setting gives more accurate and precise results for Fe, Mn and Zn (Fig. 4). Still, the correlation for Fe seems similar whether the MMR or TMR measurements are used. According to the definitions of U.S. EPA validation quality criteria when comparing field portable XRF data to an alternative analytical method [8], the data quality level for these elements is definitive Q3 based on $R^2 \geq 0.85$, RSD $\leq 10\%$. However, the calibration equation needs to be applied upon the MMR and TMR settings, since the latter results indicate $y = mx + c$ suggesting quantitative screening Q2 data quality instead of definitive Q3 if the calibration is not applied.

XRF elements detected by either MMR or TMR compared with MS data

A good linear fit with correlation coefficient of 0.9 or more is established between XRF and MS data for Al, K and Mg using the MMR setting and for Ba, Sr and Rb using the TMR setting (Fig. 5). The data quality level for these elements is definitive Q3 based on $R^2 \geq 0.85$, RSD $\leq 10\%$, and $y = x$ given the calibration is applied upon the MMR and TMR settings. Other elements that were detected both with the XRF (at TMR setting) and by MS and show a linear fit with correlation coefficient of $R^2 > 0.5$ include Th ($R^2 = 0.77$), Pb ($R^2 = 0.63$), Y ($R^2 = 0.52$) and Zr ($R^2 = 0.51$). For these elements (predominantly $R^2 < 0.70$), the data quality level is no more than qualitative screening Q1. For Mg, a quadratic fit shows a better correlation than the linear fit. Ba shows a good linear fit with a correlation

coefficient of R^2 = 0.89. However, this is mainly thanks to two samples with increased Ba concentrations. It is clear that for samples with Ba concentrations of less than 100 ppm (as measured by MS), the XRF values are not only very variable but also strongly overestimated, which is evident also from the offset of 357 ppm for the linear trend curve.

The MS data do not contain Si values, but given the significance of Si, the XRF data were compared with the values of three certified reference standards (one limestone and two dolomites). A linear fit through these three data (R^2 = 0.98) shows that Si concentrations detected by XRF (in MMR mode) show a considerable offset towards higher values compared to the certified values. The linear trend line is as follows: $Si_{XRF} = 0.391\ Si_{reference} + 1.162$.

Discussion

Optimal measurement time for XRF analyses on carbonate

The results on the relative standard deviation in function of measurement time show that the most significant improvement of the measurements' precision is from 30 to 60 seconds measurement time. Previous studies have shown that this is the case for other XRF analysers as well [33]. A measurement time of 60 seconds was suggested as best compromise between precision and measurement time for elements such as Fe, Mn, Sr, Ti and Zn [29, 33]. The most significant decrease in relative standard deviation in their studies is observed from 10 to 30 seconds measurement time, and hence, falls outside the tests of our study where the minimum measurement time was 30 seconds. Portable XRF studies on obsidian, for example, over the last four years show a wide variety in terms of measurement time, ranging from 10 to 360 seconds [2, 12-16, 34-36]. Most of these studies, however, do not present actual tests of how precision and accuracy of the XRF measurement is influenced by the measurement time. For this study, and thus the calibration for the application of XRF on carbonate, a measurement time of 120 seconds on each, the MMR and TMR, setting was taken. However, future studies can consider a measurement time of 60 seconds as good compromise between productivity and precision.

Impact of sample preparation on XRF measurements

A comparison of 4µm Prolene thin film with 2µm Mylar thin film in this study showed differences for Si and S, with higher concentrations using the Mylar film than the Prolene film, and for V, with concentrations a few ppm higher using the Prolene film compared to the Mylar film. Trace contamination of S in the Mylar thin films has also been reported before [29]. The impact of thin film on the decrease of the signal is highlighted by Forster et al. [30] who reported that Mylar film absorbs 80% of Si fluorescent intensity. X-ray absorption varies with different filter materials and increases with filter thickness; an on-line calculator can be found for example at henke.lbl.gov/optical_constants/filter2. In addition, we would not recommend the use of 1.5µm thin film in terms of practicality as it tears very easily when mounting the sample cups and electrostatic charging makes handling this film quite difficult.

The impact of different grain sizes did not show any consistent changes in elemental concentrations, except for Ba and Sr, where the concentration is lower for the coarser size fraction. A previous study has shown that a reduction in particle size of calcium-magnesium carbonate samples causes a reduction in the intensities of Fe, S and K, but an increase in the intensities of Ca and Si [25]. These differences in concentrations were not observed anymore when the particle size was smaller than 325 mesh, which equals 44µm [25]. These observations are thus not consistent with the fact that most of the elements have similar concentrations in the 63-125 and 125-250µm size fractions in our study. This could be linked to the much improved handheld XRF instrument used in our study compared to the one in the mentioned study of 1999. The impact of grain size in hand samples (non-destructive) rather than in powder, has also been tested in previous studies, that demonstrated that more replicates were needed for coarse-grained rocks, such as granite, than for fine-grained rocks, such as clay, to obtain the same precision [30].

Different sample preparation can impact on the elemental concentration in the samples. Most distinct differences are seen for Mg, where polished samples clearly show higher concentrations measured by XRF compared to that in fresh rough rock surface and lowest concentrations are found in weathered rock surfaces. Mg is one of the most difficult elements to detect by XRF because of its light atomic weight, and hence, the roughness of the sample, and thus the distance of the beam through non-

vacuum can play a significant role, which we interpret here as the explanation for the observed lower Mg concentrations in fresh rock surfaces compared to polished rock surfaces. Similarly, the Mg concentration in powder samples (which may contain some air between the particles) show lower concentrations by XRF compared to that measured on polished rock surfaces. The latter difference could also be explained, though, by the fact that for powders, a thin film sits between the powder and the XRF, in contrast to the polished samples which sit directly on the XRF. The presence of thin film decreases the fluorescence signal, which most significantly impacts light elements [30]. Finally, the weathered rocks surfaces have the lowest Mg concentrations and this is probably the combined effect of some air between the sample and the instrument (as is the case for fresh rough rock surfaces) as well as the effect of weathering (alteration) of the surface, which led to a decrease in the Mg content. In a similar way, also the Ca content is lower in the weathered rock surface than for fresh rough and polished samples, which we also ascribe to weathering. Another effect of weathering seems to be an increase in both Al and Ti in the weathered surface. The effects for Fe and Mn are not completely conclusive, but seem to suggest higher values for fresh and weathered rock surfaces than for polished and powder samples. The impact of weathering has been documented by portable XRF on dolerite and rhyolite outcrops, where generally depletions in Ca, Fe and Y were observed in weathered surface layers in dolomite, in contrast to K and Pb that were enriched [37]. No significant changes were observed in K or Y and Pb (which were generally very low) in our study. Also Forster et al. [30] show that surface irregularities strongly affect measurements of light elements such as Si, Ca and Ti, whereas heavy elements like Rb, Sr and Zr are not much influenced. Still, accuracy is possible within about 10%, and often better, for elements with atomic number higher or equal to 26 (Fe) in samples with relatively shallow irregular surface structures [30].

As mentioned above, the impact of the irregularity of the surface is minimal for most elements in this study, except for Mg. Previous studies investigating the impact of the XRF measurement by the irregularity of the surface presented a correction factor to take account of the scatter peak intensity due to the air gap associated with the surface irregularity [31]. However, the corrections were only presented for elements with an atomic weight of 56 or higher [31], and thus not for the lighter elements,

such as magnesium. Our results do not show that a correction is needed for the heavier elements with the current type of XRF used in our study.

Applicability of handheld XRF spectrometry in carbonate studies

Previous studies investigated the performance of different types of portable XRF instruments to test precision and accuracy of analyses on a range of materials [29, 34, 38]. Portable XRF instrument stability is reported to be generally good in the time range of one month [34], but detection deteriorates after two to five months [38]. These studies also showed that performance is highly variable between instruments [29] and that qualitative chemical data are generally precise but very inaccurate [34, 38]. Therefore, a calibration procedure appropriate to the material analysed needs to be established for each instrument [38]. As far as the authors are aware of, the current paper presents the first calibration for handheld XRF spectrometry on carbonate.

This study provides correction equations for the quantification of Ca, Ti, Fe, Mn, Zn, Al, K, Mg, Ba, Sr, Rb and Si in carbonate (Table 2) to apply onto the values obtained at TMR and MMR modes provided by the manufacturer. Quantification and calibration of these elements, in contrast to some other elements, was possible because the measured values in at least part of the samples was 10 times or more higher than the detection limit, considered as essential for quantification [39]. For all elements with good correlation between MS and XRF, a linear trend line is the best fit. However, for Mg a quadratic trend line seems to have a slightly better fit than the linear trend line.

The portability and flexibility of the handheld XRF provides the opportunity of making measurements in situ which could save time and costs than when samples need to be collected in the field, shipped and then afterwards being analysed in the lab. In situ measurements are good for defining rapidly sites of highest interest, and thus can help making decisions while being the field. As explained above, such in situ measurements do come with some challenges, such as the impact of surface irregularities and weathering of the rocks. In studies on carbonate, weathering is a significant challenge, given the chemical reaction of dissolution of carbonate with acidic rain water. This study has shown significant decreases in the Ca and Mg content in the weathered surface of exposed carbonate rocks. Moreover, as can be observed in many outcrops, weathering of the rock surface will vary significantly across

outcrops, due to for example blocks of rocks that fell off the cliff face more recently than others, and the impact of water circulation running down cliff faces or slopes, which will not be equal across the outcrops. Hence, measuring elemental concentrations on weathered outcrops, even with the scope of looking for relative trends rather than absolute values is not advised for carbonate studies. However, the impact of the roughness of the samples was minimal for most elements (except for magnesium). Hence, we suggest that field work in situ could take place on site, but only by hammering rock chips of the cliff face and measuring parts of the rock that are not affected by weathering. In addition, depending on safety precautions taken with respect to the X-ray source of the instrument and the fact that scatter from X-rays can occur with open beam on irregular rock surfaces, XRF measurements will be slowed down if one uses a tripod to keep the researcher away from the X-ray scatter during measurement. Setting up the tripod for each new measurement takes a significant amount of time compared to just holding the instrument. Given these two facts, a good compromise may be to use the XRF on its stand with closed beam on hammered rock samples. This procedure would not be much different in the lab or in the field, but being able to do this in the field does come with significant advantages of having good measurements on site during the field work period, which may be important for making decisions on site.

Conclusion

The handheld ED-XRF allows rapid, quantitative analyses (of definitive Q3 data quality) of Ca, Ti, Fe, Mn, Zn, Al, K, Mg, Ba, Sr, Rb and Si on carbonate rocks, provided appropriate corrections (as presented in this study) are applied to the manufacturer's calibration based on a series of carbonate standards. A measurement time of 60 seconds on both MMR and TMR modes is suggested for accurate measurements of elemental concentrations in carbonate samples. Our results have shown that grain size in powders and roughness of hand samples do not impact significantly on measured elemental concentrations, except for the light element magnesium. In contrast, weathering of carbonate rock surfaces does pose a significant issue, especially with respect to elemental concentrations of Ca, Mg, Ti and Al. One should be cautious with using handheld XRF on weathered

outcrops since even relative trends in elemental concentrations could be unreliable due to varying degrees in weathering across the studied outcrop. This issue can be overcome by hammering fresh rock chips from the outcrop, and measure those on site. This would still provide the advantage of obtaining values as field work proceeds, which can be hugely advantageous.

Acknowledgements

The authors gratefully acknowledge the agencies that provided funding for this project. The first author was awarded a BP UROP bursary and the second author was awarded Imperial College London departmental UROP matching funds for this research project. The XRF equipment was funded by Qatar Petroleum, Shell and the Qatar Science and Technology Park. The authors are indebted to Ross Morgan, who has been an enormous help in the set-up of the safety protocols and documents for handling the XRF. Mike Dobby (Bruker) is kindly thanked for advice on using the XRF. Part of the samples used in this study were collected and characterized during previous research projects in the Qatar Carbonates and Carbon Storage Research Center funded by Qatar Petroleum, Shell and the Qatar Science and Technology Park (QSTP). Rudy Swennen (Katholieke Universiteit Leuven) is acknowledged for providing a set of dolomite samples for analysis. This research also used samples provided by the Integrated Ocean Drilling Program (IODP) and the International Continental Scientific Drilling Program (ICDP). We thank the IODP and ICDP Core Repository staff as well as the Scientific Party of the IODP 143, 194 and ICDP FARDEEP Expeditions. Three anonymous reviewers and the editor are thanked for their constructive comments which improved this manuscript.

Figure captions

Fig. 1. Measurement quality in function of measurement time evaluated for XRF analyses (using MMR setting) on certified dolomite reference standard JDo-1. The reference material was measured as powder in a sample cup covered by 4μm thin Prolene film. A. Average standard error of triplicate XRF measurements in function of measurement time, reported for elements Ca, Mg, Si, Mn and Fe.

Standard error decreases with increasing measurement time. B. Reproducibility of triplicate XRF measurements, expressed as percentage relative standard deviation (of triplicate measurements) in function of measurement time, reported for elements Ca, Mg, Si, Mn, Fe and Zn. Element concentration is stated in brackets next to the element name.

Fig. 2. Comparison of XRF measurements on samples prepared in different ways (polished with silicon carbide grit 600, grit 220, fresh rough hammered surface and weathered rock surface) with XRF measurements on powder of the same samples. Ca, Mg, Al were measured at the MMR setting, whereas Fe, Mn and Sr were measured at the TMR setting. Linear fit trend lines are presented.

Fig. 3. Comparison of elemental concentrations measured by MS and XRF (using MMR and TMR settings) with the certified reference values for certified limestone reference standard CRM No. 393 (A) and certified dolomite reference standard GBW 07114 (B). Reported elements for the limestone standard include Ca, Fe, Mg, Mn, Sr and in addition Al and Ba for MS and K for XRF. Reported elements for the dolomite standard include Ba, Ca, Cu, Fe, Mg, Mn, Ni, Sr, Zn, Th, U, Zr and in addition Al, Ce, Dy, Er, La, and Sm for MS and Cr, K and V for XRF. Linear best fit curves (forced through 0) are presented on the graphs.

Fig. 4. XRF measurements of Ca, Ti, Fe, Mn and Zn concentrations using both MMR and TMR settings in function of MS data of the series of selected certified and internal standards as listed in Table 1. Best fit linear trend curves are presented with correlation coefficient. Best fits in terms of precision and accuracy correspond to MMR data for Ca and Ti and TMR data for Fe, Mn and Zn.

Fig. 5. XRF measurements of Al, K and Mg using the MMR setting and of Ba, Sr and Rb using the TMR setting in function of MS data of the series of selected certified and internal standards as listed in Table 1. Best fit linear trend curves are presented with correlation coefficient. For Mg, also a quadratic trend curve is presented which has a better correlation coefficient than that of the linear trend curve.

Tables

Table 1. Details of 38 standards used for cross-validation. Details on the age and origin/locality of the standards are presented.

Table 2. Correction equations to convert XRF measured values (x) to absolute concentrations (y). Coefficients presented for equation $y = a\ x^2 + b\ x + c$. Note that some elements are reported in %, whereas others are in ppm concentrations.

References

1. G. J. Weltje and R. Tjallingii, *Earth and Planetary Science Letters*, 2008, **274**, 423-438.
2. E. Frahm, *Journal of Archaeological Science*, 2013, **40**, 1080-1092.
3. Z. Yuan, Q. Cheng, Q. Xia, L. Yao, Z. Chen, R. Zuo and D. Xu, *Geochemistry-Exploration Environment Analysis*, 2014, **14**, 265-276.
4. D. C. Arne, R. A. Mackie and S. A. Jones, *Geochemistry-Exploration Environment Analysis*, 2014, **14**, 233-244.
5. V. Crupi, A. Giunta, B. Kellett, F. Longo, G. Maisano, D. Majolino, A. Scherillo and V. Venuti, *Analytical Methods*, 2014, **6**, 6301-6309.
6. M. Gemelli, M. D'Orazio and L. Folco, *Meteoritics & Planetary Science*, 2014, **49**, A132-A132.
7. F. L. Melquiades and C. R. Appoloni, *Journal of Radioanalytical and Nuclear Chemistry*, 2004, **262**, 533-541.
8. C. Parsons, E. Margui Grabulosa, E. Pili, G. H. Floor, G. Roman-Ross and L. Charlet, *Journal of Hazardous Materials*, 2013, **262**, 1213-1222.
9. B. Lemiere, V. Laperche, L. Haouche and P. Auger, *Geochemistry-Exploration Environment Analysis*, 2014, **14**, 257-264.
10. A. Ene, A. Bosneaga and L. Georgescu, *Romanian Journal of Physics*, 2010, **55**, 815-820.
11. C. Vanhoof, V. Corthouts and K. Tirez, *Journal of Environmental Monitoring*, 2004, **6**, 344-350.
12. A. J. Nazaroff, K. M. Prufer and B. L. Drake, *Journal of Archaeological Science*, 2010, **37**, 885-895.
13. J. K. Millhauser, E. Rodriguez-Alegria and M. D. Glascock, *Journal of Archaeological Science*, 2011, **38**, 3141-3152.
14. M. Golitko, J. Meierhoff and J. E. Terrell, *Archaeology in Oceania*, 2010, **45**, 120-129.
15. K. P. Freund and R. H. Tykot, *Archaeological and Anthropological Sciences*, 2011, **3**, 151-164.
16. E. Frahm, B. A. Schmidt, B. Gasparyan, B. Yeritsyan, S. Karapetian, K. Meliksetian and D. S. Adler, *Journal of Archaeological Science*, 2014, **41**, 333-348.
17. R. B. Scott, A. J. Shortland, P. Degryse, M. Power, K. Domoney, S. Boyen and D. Braekmans, *Glass Technology-European Journal of Glass Science and Technology Part A*, 2012, **53**, 65-73.
18. S. Liu, Q. H. Li, Q. Fu, F. X. Gan and Z. M. Xiong, *X-Ray Spectrometry*, 2013, **42**, 470-479.
19. S. Liu, Q. H. Li, F. Gan, P. Zhang and J. W. Lankton, *Journal of Archaeological Science*, 2012, **39**, 2128-2142.

20. K. Tantrakarn, N. Kato, A. Hokura, I. Nakai, Y. Fujii and S. Gluscevic, *X-Ray Spectrometry*, 2009, **38**, 121-127.
21. Z. Petrova, J. Jehlicka, T. Capoun, R. Hanus, T. Trojek and V. Golias, *Journal of Raman Spectroscopy*, 2012, **43**, 1275-1280.
22. T. W. Dahl, M. Ruhl, E. U. Hammarlund, D. E. Canfield, M. T. Rosing and C. J. Bjerrum, *Chemical Geology*, 2013, **360**, 241-251.
23. H. Rowe, N. Hughes and K. Robinson, *Chemical Geology*, 2012, **324**, 122-131.
24. R. Figi, O. Nagel, M. Tuchschmid, P. Lienemann, U. Gfeller and N. Bukowiecki, *Analytica Chimica Acta*, 2010, **676**, 46-52.
25. B. D. Wheeler, in *Masonry: Materials, Testing, and Applications*, eds. J. H. Brisch, R. L. Nelson and H. L. Francis, 1999, vol. 1356, pp. 34-61.
26. A. J. Hutchinson, J. B. Johnson, G. E. Thompson, G. C. Wood, P. W. Sage and M. J. Cooke, *Atmospheric Environment Part a-General Topics*, 1992, **26**, 2785-2793.
27. A. J. Hutchinson, J. B. Johnson, G. E. Thompson, G. C. Wood, P. W. Sage and M. J. Cooke, *Atmospheric Environment Part a-General Topics*, 1992, **26**, 2795-2803.
28. P. A. Warke, J. M. Curran, A. V. Turkington and B. J. Smith, *Building and Environment*, 2003, **38**, 1113-1123.
29. G. E. M. Hall, G. F. Bonham-Carter and A. Buchar, *Geochemistry-Exploration Environment Analysis*, 2014, **14**, 99-123.
30. N. Forster, P. Grave, N. Vickery and L. Kealhofer, *X-Ray Spectrometry*, 2011, **40**, 389-398.
31. P. J. Potts, P. C. Webb and O. WilliamsThorpe, *Journal of Analytical Atomic Spectrometry*, 1997, **12**, 769-776.
32. R. J. Speakman, N. C. Little, D. Creel, M. R. Miller and J. G. Inanez, *Journal of Archaeological Science*, 2011, **38**, 3483-3496.
33. P. S. Ross, A. Bourke and B. Fresia, *Geochemistry-Exploration Environment Analysis*, 2014, **14**, 171-185.
34. N. Goodale, D. G. Bailey, G. T. Jones, C. Prescott, E. Scholz, N. Stagliano and C. Lewis, *Journal of Archaeological Science*, 2012, **39**, 875-883.
35. P. W. Jia, T. Doelman, C. Chen, H. Zhao, S. Lin, R. Torrence and M. D. Glascock, *Journal of Archaeological Science*, 2010, **37**, 1670-1677.
36. P. J. Sheppard, G. J. Irwin, S. C. Lin and C. P. McCaffrey, *Journal of Archaeological Science*, 2011, **38**, 45-56.
37. P. J. Potts, F. Bernardini, M. C. Jones, O. Williams-Thorpe and P. C. Webb, *X-Ray Spectrometry*, 2006, **35**, 8-18.
38. N. W. Brand and C. J. Brand, *Geochemistry-Exploration Environment Analysis*, 2014, **14**, 125-138.
39. D. J. Kalnicky and R. Singhvi, *Journal of Hazardous Materials*, 2001, **83**, 93-122.

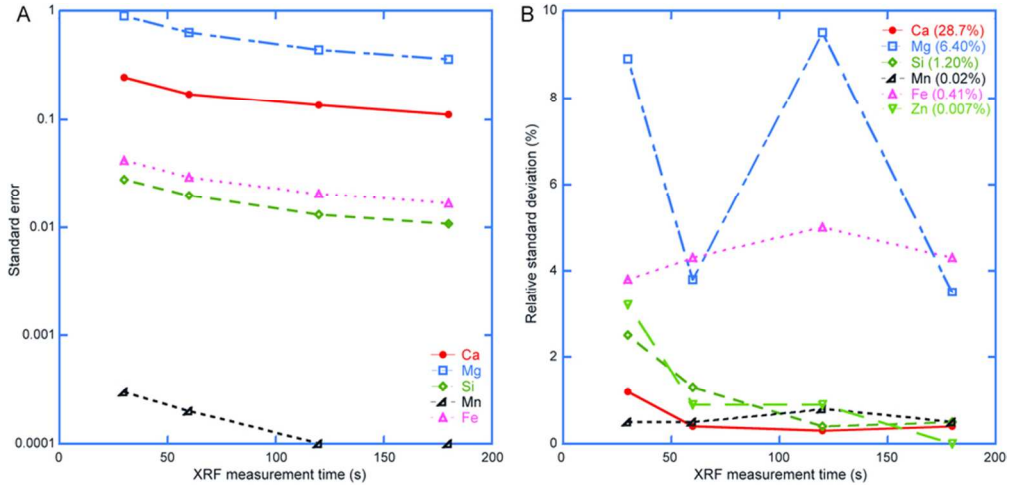

80x38mm (300 x 300 DPI)

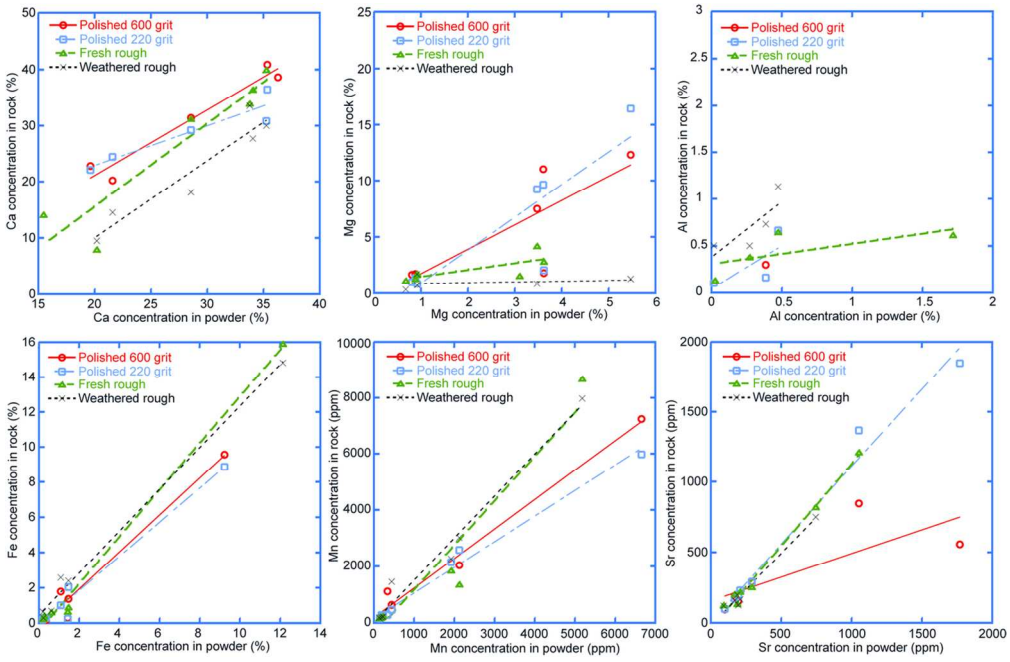

118x77mm (300 x 300 DPI)

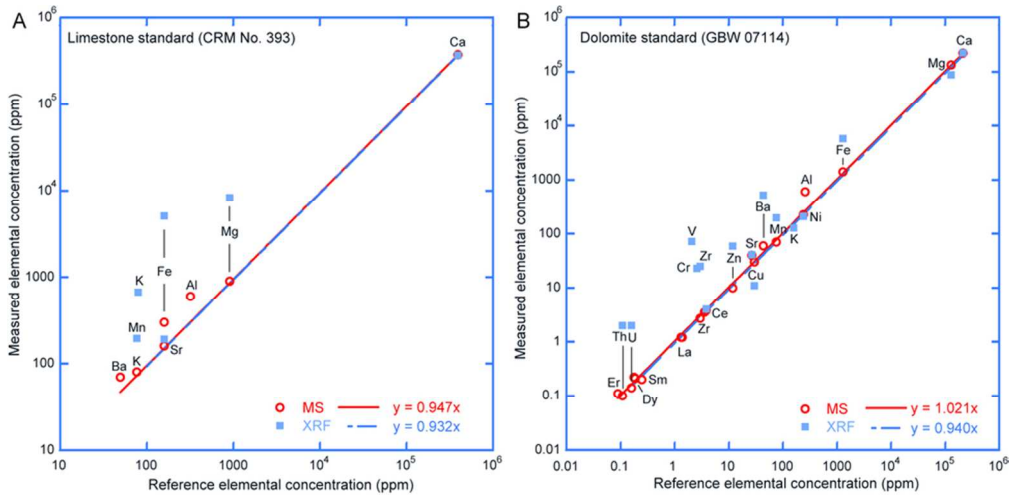

81x39mm (300 x 300 DPI)

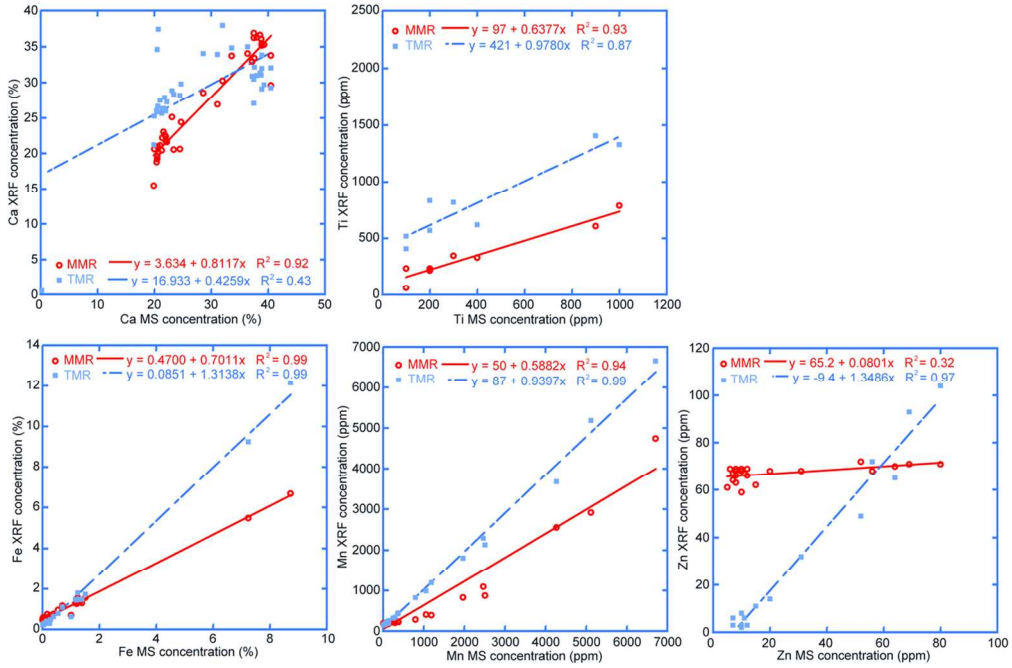

118x77mm (300 x 300 DPI)

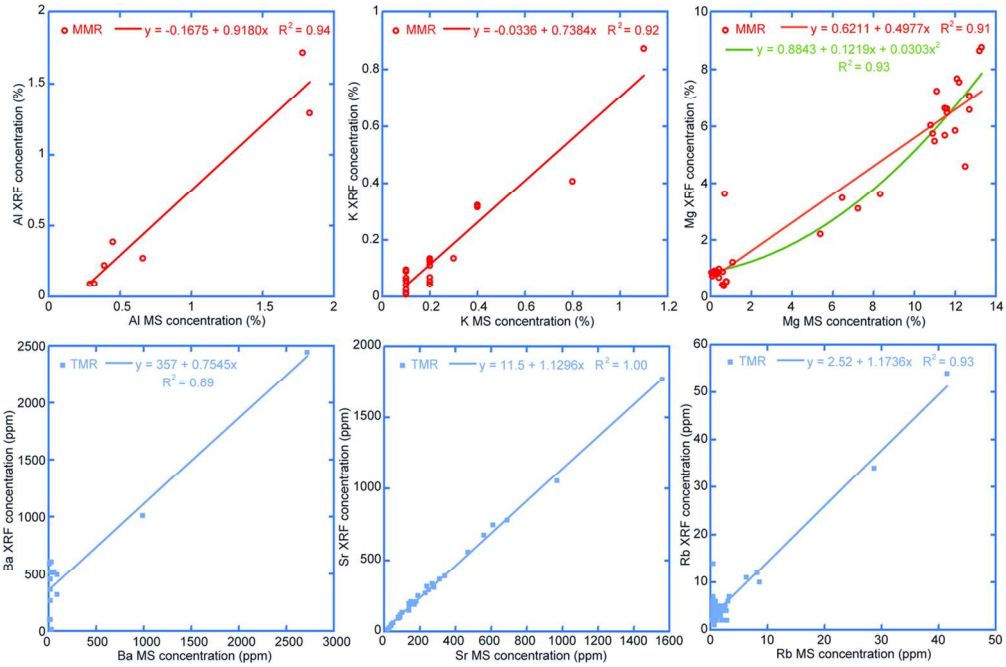

117x77mm (300 x 300 DPI)

Table 1. Details of 38 standards used for cross-validation. Details on the age and origin/Locality of th

Name	Sample type	Location
GBW 07114	Certified dolomite standard	
CRM No. 393	Certified limestone standard	
FD 53.55	Limestone	ICDP 10B Fennoscandia Arctic Russia – Drilling Early Earth Project
FD 257	Dolomite	ICDP 10B Fennoscandia Arctic Russia – Drilling Early Earth Project
143-161BD	Dolomite	Resolution Guyot atoll, Mid-Pacific Mountains
143-133WD	Dolomite	Resolution Guyot atoll, Mid-Pacific Mountains
194-18D	Dolomite	Marion Plateau
143-131L	Limestone	Resolution Guyot atoll, Mid-Pacific Mountains
143-161L	Limestone	Resolution Guyot atoll, Mid-Pacific Mountains
194-27L	Limestone	Marion Plateau
JM2F6	Calcite	Jebel Madar, Oman
JMF6B	Calcite	Jebel Madar, Oman
BAB1	Limestone	Wadi Bani Awf, Jebel Akhdar, Oman
MD44	Dolomite	Wadi Mistal, Jebel Akhdar, Oman
SALIL	Limestone	Jebel Madar, Oman
AK32	Dolomite	Wadi Sahtan, Jebel Akhdar, Oman
MPA7	Limestone	Wadi Mistal, Jebel Akhdar, Oman
JM2E12	Calcite	Jebel Madar, Oman
MAD64	Barite	Jebel Madar, Oman
FD-	Dolomite	Fuente Dé, Picos de Europa, Spain
JMA26	Limestone	Jebel Madar, Oman
MPA35	Early diagenetic dolomite	Wadi Mistal, Jebel Akhdar, Oman
MPA17	Late diagenetic dolomite	Wadi Mistal, Jebel Akhdar, Oman
MC29	Late diagenetic dolomite	Wadi Mistal, Jebel Akhdar, Oman
JM2A16	Limestone	Jebel Madar, Oman
MC14	Late diagenetic dolomite	Wadi Mistal, Jebel Akhdar, Oman
BAH12	Late diagenetic dolomite	Wadi Bani Awf, Jebel Akhdar, Oman
MA38	Limestone	Wadi Mistal, Jebel Akhdar, Oman
RAYDA	Limestone	Jebel Madar, Oman
FD-1	Limestone	Fuente Dé, Picos de Europa, Spain
BM1	Dolomite with anhydrite	Brightling Mine, East Sussex, UK
RS11	Dolomite	Ranero, Spain
RS8	Dolomite	Soumagne core, Belgium

RS2	Dolomite	Field, British Columbia, Canada
RS1	Dolomite	Hastenrath, Germany
RS13	Dolomite	Bow Valley, British Columbia, Canada
S20L	Limestone	S20 core, Southern Mallorca
S20D	Dolomite	S20 core, Southern Mallorca

ıe standards are presented.

Age
Paleoproterozoic
Paleoproterozoic (host rock)
Cretaceous (host rock)
Cretaceous (host rock)
Miocene (host rock)
Cretaceous
Cretaceous
Miocene
Cretaceous (host rock)
Cretaceous (host rock)
Khufai Fm., Ediacaran
Sahtan Group, Jurassic (host rock)
Salil Fm., Cretaceous
Saiq Fm., Permian (host rock)
Saiq Fm., Permian
Cretaceous (host rock)
Cretaceous (host rock)
Valdeteja Fm., Carboniferous (host rock)
Habshan Fm, Cretaceous
Saiq Fm, Permian (host rock)
Saiq Fm, Permian (host rock)
Sahtan Group, Jurassic (host rock)
Shuaiba Fm, Cretaceous
Sahtan Group, Jurassic
Khufai Fm, Ediacaran
Sahtan Group, Jurassic
Rayda Fm, Cretaceous
Valdeteja Fm., Carboniferous
Jurassic (host rock)
mid Cretaceous (host rock)
Mississippian (host rock)

Cambrian (host rock)
Mississippian (host rock)
Devonian (host rock)
Miocene
Miocene (host rock)

Table 2. Correction equations to convert XRF measured values (x) to absolute concentrations (y). Coefficients

Element	Setting	a	b	c	R^2
Al (%)	MMR	0	1.0205	0.22254	0.93686
Ba (ppm)	TMR	0	1.1768	-391.34	0.88788
Ca (%)	MMR	0	1.128	-1.6462	0.91562
Fe (%)	TMR	0	0.75425	-0.0562	0.99096
K (%)	MMR	0	1.2422	0.062473	0.91729
Mg (%)	MMR	-0.15385	3.0743	-1.8388	0.93367
Mn (ppm)	TMR	0	1.0569	-85.218	0.99312
Rb (ppm)	TMR	0	0.79107	-1.7254	0.92838
Si (%)	MMR	0	2.5093	-2.9115	0.98002
Sr (ppm)	TMR	0	0.8825	-9.3669	0.99687
Ti (ppm)	MMR	0	1.4607	-114.52	0.9315
Zn (ppm)	TMR	0	0.71989	7.6621	0.97086

presented for equation y = a x^2 + b x + c. Note that some elements are reported in %, whereas others in ppm concen

ıtrations.